

### EEG Signal Analysis for Dyslexia Prediction Using Deep Learning Techniques

# Dr.Vishal Patil<sup>1</sup>,Dr.Bajirao Shirole<sup>2</sup>, Dr.Rajiv R.Bhandari<sup>3</sup>, Dr. Sharmila Zope<sup>4</sup>,M.D.Sanap<sup>5</sup>,Dr.Vijay More<sup>6</sup>,Vijay Bodake<sup>7</sup>, Dr.R. Ramkumar<sup>8</sup>

<sup>1</sup>Associate Professor, Department of AIML, Loknete Gopinathji Munde Institute of Engineering Education & Research, Email ID:vp0106@gmail.com

<sup>2</sup>Associate professor, Department of Computer Engineering, Loknete Gopinathji Munde Institute of Engineering Education & Research,

Email ID:.baji.shirole@gmail.com

<sup>3</sup>Associate Professor, Department of Computer Engineering ,SNJB,s Late Sau. K. B. Jain College of Engineering Chandwad Email ID:.<u>rajivrbhandari@gmail.com</u>

<sup>4</sup>Assistant Professor, Department of Computer, Jawahar Education Society's Institute of Technology, Management and Research, Nashik. <a href="mailto:sharmila.zope@gmail.com">sharmila.zope@gmail.com</a>

<sup>5</sup>Assistant Professor, Department of AIML, Loknete Gopinathji Munde Institute of Engineering Education & Research, Email ID. sanapmd@gmail.com

<sup>6</sup>Associate Professor, Department of Computer Engineering, MET's Institute of Engineering, Bhujbal Knowledge City,

Email ID vbmore2005@rediffmail.com

<sup>7</sup>Assistant Professor, Department of computer engineering, Loknete Gopinathji Munde Institute of Engineering Education & Research,

Email ID. vijaybodake@gmail.com

<sup>8</sup>Associate Professor,School of Engineering and Technology, Department of Electrical and Electronics Engineering,Dhanalakshmi Srinivasan University,Trichy,Tamilnadu,India.

Email ID 2019ramkr@gmail.com

Cite this paper as:Dr.Vishal Patil1, Dr.BajiraoShirole ,Dr.RajivR.Bhandari,Dr. SharmilaZope,M.D.Sanap ,Dr.Vijay More,Vijay Bodake, Dr.R.Ramkumar, (2025) EEG Signal Analysis for Dyslexia Prediction Using Deep Learning Techniques. *Journal of Neonatal Surgery*, 14 (27s), 196-206.

#### **ABSTRACT**

Dyslexia, a specialized learning condition, affects around 10% of the global population. Adding audio to printed text may produce duplication, but it may be advantageous for kids with dyslexia who need help reading. Studying both the learning process and the learning results in kids with and without dyslexia can shed light on this problem and assist in determining if the redundancy effect is constrained. Most prior electroencephalogram (EEG) tests on people with and without dyslexia identified disparities in the challenges of those with dyslexia. In this study, we provide a model for predicting readers with and without dyslexia based on EEG signals from the brain obtained with BrainSensor equipment. This article treats signals using Empirical Mode Decomposition (EMD) and Singular Spectrum Analysis (SSA). After that, these output signals are given to Deep Forest Classifier to predict dyslexia students. The experiments are carried out on collected signals and validated its performance using four parameters: Accuracy, recall, precision, and F-measure. The proposed model is compared with five existing Machine Learning (ML) and Deep Learning (DL) techniques implemented with SSA-EMD, SSA, and EMD for performance analysis. The proposed Deep Forest Classifier (DFC) model performs better while executing both SSA-EMD and yields 98% accuracy.

**Keywords:** Dyslexia, Deep Forest Classifier, Empirical Mode Decomposition, Electroencephalogram, Singular Spectrum Analysis, Machine Learning.

#### 1. INTRODUCTION

Based on graph theory, the study of compound networks has been smeared in various domains, including social sciences, physics, and information technology. The breakthroughs have been applied to neuroscience and understanding complex networks originating in the brain. Furthermore, it provides a strong method of measuring the structural and functional.

MRI (fMRI), EEG, and MEG. Complex network analysis, in this sense, aids in quantifying brain networks using a small sum of neurobiologically important and easily computed variables. This is an excellent setting for investigating structural—functional connection links in brain functions. As a result, it is a potential approach for detecting aberrant connections in neurological and mental illnesses [2].

Many examples in the literature of using complex network analysis to investigate brain network characteristics. For example, the analysis of complex networks from physiological and pathological brain aging such as Alzheimer's disease in [3, 4, 5, 6]. Other studies employ functional connectivity and complex network analysis for neurological disorders like epilepsy and schizophrenia. [7] use sophisticated networks to identify variations in EEG-based practical connectivity patterns. Other studies, such as [8], use theoretical graph analysis to explore schizophrenia using MEG functional connectivity networks. We provide some known research on functional network connection and structure in Developmental Dyslexia in this perspective (DD). The application of EEG signals is becoming increasingly widespread. The authors of [9] used graph analysis to investigate variations in the topological features of functional networks. In [10], EEG connectivity research was performed to determine if defective connection scales with the extent of reading dysfluency. In this sector, [11] calculated Phase-Amplitude Coupling to assess the correctness of low-frequency speech envelope encoding.

DD is a neurological condition that causes learning disability disorders and affects between 5% and 13% of the population [12]. DD diagnosis is a relevant study area that benefits from applying complex network analysis. Within this topic, early diagnosis is receiving increasing attention. It is an essential task to help dyslexic children have proper personal development by applying preventive strategies for teaching language. For this purpose, EEG signals enable specific measures not associated with reading for an impartial and early diagnosis in pre-readers subjects.

#### Related works

In Table I, a study of existing works is described along with a total number of subjects and performance analysis.

#### Proposed System

This section briefly explains the proposed method. Fig. 1 shows the working flow of the proposed methodology that has preprocessing, singular spectrum analysis, EMD, and DFC classification with performance evaluation. Here, we have collected the data from 15 students with reading issues, normal category people, and visually challenged people using three different nodes such as C3, C4, and CZ. Once the data is collected, it will go for pre-processing analysis. Then, spectrum analysis and EMD process are used for signal processing, and these outputs are given to the deep forest classifier for final prediction.

### Signal pre-processing

Blinking eyes and movement-induced impedance variations were reduced in the EEG data through pre-processing. Independent Component Analysis (ICA) removes distortions such as eye blinking signals from EEG data [18]. Each channel's EEG input is then normalized to have a zero mean and unit variance to ensure that the scale is uniform in the future (for instance, Power Spectral Density calculation). Small samples were removed from the beginning and end of the signals to ensure that each person received the same number of samples. Each subject and experiment received 136 seconds of EEG recording. As an aside, these 136-second signals were split into 40-second segments to expedite the post-processing procedure (such as SSA computation). A recording time of 40 seconds allows for good frequency precision at the lowest possible EEG frequency, equivalent to the Delta band ([0.5-4] Hz). Finally, all segments are subjected to a band-pass filter to remove all except the most relevant frequencies ([0.5, 40] Hz). Each segment is processed independently to generate data for the classifier's training.

TABLE I. COMPARATIVE ANALYSIS OF EXISTING TECHNIQUES.

Author Year	Objective	No. of subjects used in the works	Method of data analysis	Performances
H. M. Al- Barhamtoshy and D. M. Motaweh [13]	Using a computational analytic classifier to detect dyslexia early on	80	The data pieces were clustered using machine learning methods based on feature similarities.	K-means 89.6% ANN 89.7% Fuzzy 85.7%

H. Perera et.al [14]	To investigate the efficacy of a ML techniquecalled Support Vector Machine (SVM)indetecting dyslexia using brain signals gathered during writing and typing.	32	Using Cubic SVM, a classifier was built for recognizing activation patterns from the processed EEG data.	Accuracy =78.2% Specificity=66.7% Sensitivity=88.2%
JothiPrabha and R. Bhargavi [15]	To present a prediction model for distinguishing dyslexics from non-dyslexics based on eye moment.	185	SVM-PSO, a hybrid kernel based on PSO, was used to predict dyslexia using high-level characteristics retrieved by PCA.	Accuracy: SVM-PSO 95% Linear SVM 90%
Frid and L. M. Manevitz [16]	Using machine learning, compare the ERP signals of dyslexic and proficient readers.	32	SVM ANN and PCA are used for the prediction process.	Accuracy 78.0%
Karim et.al [17]	To sense dyslexia marker from brain activity signal composed during resting stage using Multi-Layer Perceptron (MLP)	6	MLP was utilized to differentiate dyslexic brain function.	Accuracy: Eye closed 85.0% Eye opened 86.0%
Z Cui et.al[21]	To measure the multidimensional effect of developmental dyslexia on WM connectivity of the human brain using Linear Support Vector Machine(LSVM)	61	LSVM classifier using combined VM features	Accuracy = 83.61 % Sensitivity = 75 % Specificity = 90.91 %
AZA Zainuddin et.al [22]	To identify types of dyslexia from EEG signals during writing.	54	ML classifiers such as KNN, SVM and ELM, and DL utilized LSTM to attain the highest classification accuracy in distinguishing between poor dyslexic, capable dyslexic and normal children based	Accuracy: KNN – 81.67 % SVM – 88.33% ELM – 81.67%

			on EEG signals during writing-related tasks.	
P Tamboer et.al [23]	To classify individual structural neuro-imaging scans of students with and without dyslexia	49	SVM	Accuracy = 80% Sensitivity = 82% Specificity = 78%
S Kaisar,& Chowdhury[24]	To detect Dyslexia using an Ensemble-based machine learning technique.	3644	Ensemble-based machine learning technique	Accuracy = 80.61 - 83.52%

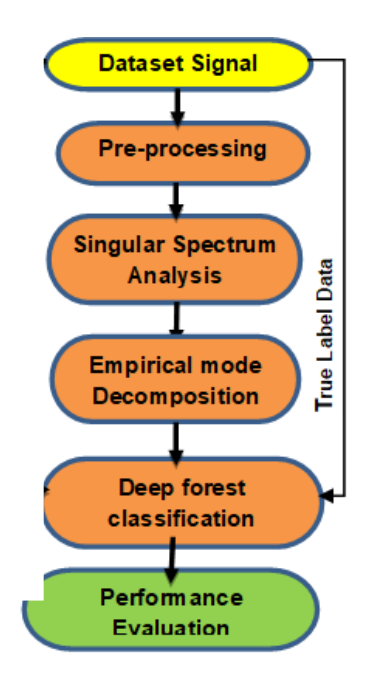


Fig. 1. Proposed Model.

### Singular Spectrum Analysis

When using SSA, the original time series is broken down into a total of K different series, each of which is estimated using a different spectral estimator. According to mathematical theory, an L-lagged series X = 1 to N is embedded in a K-dimensional vector space containing the covariance matrices' eigenvectors. The following is the definition of  $x_i$ , lag vectors:

$$\bar{X}_i = \{x_i, \dots, x_{i+L-1}\} \in R^L$$
 (1)

where K = N - L + 1. Thus, the covariance matrix.

$$X_{x} = \frac{1}{N-L} \sum_{t=1}^{N-L} \overline{X(t)X(t+L)}$$
 (2)

The temporal empirical orthogonal functions are the K eigenvectors  $E_k$  of the lag-covariance matrix C x (EOFs). Furthermore, the eigenvalues  $E_k$  corresponding to each eigenvector explanation for the direction  $E_k$  contribution to the total variance. As a result, the projection of the unique time series on the k-component may be calculated as:

$$Y_k = \bar{X}(t+n-1)E_k(n) \tag{3}$$

Each SSA component accounts for a portion of the variation in the original signal. When these components are arranged by their corresponding eigenvalues, the first mechanisms account for greater variation than later components. However, as seen in Fig. 2, several recovered components are significantly connected. These connected components can be grouped without affecting their interpretability.

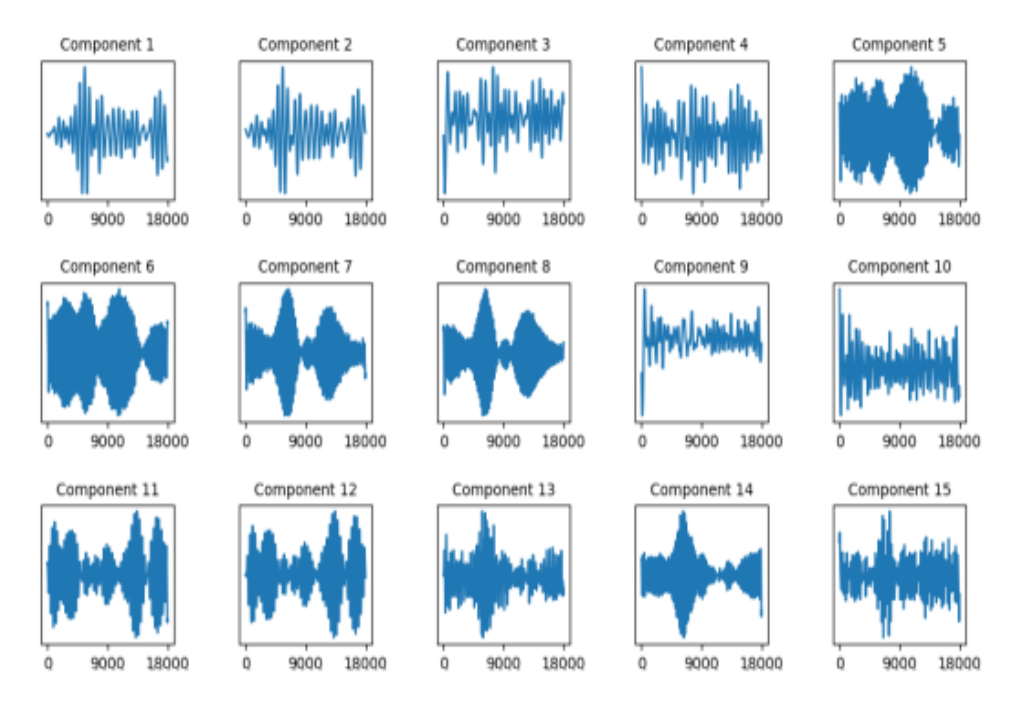


Fig. 2. Sample of 15 first SSA components removed for channel 0.

#### **EMD**

The EMD [19] breaks any signal in the time domain into a group of AM-FM modules regardless of whether the signal is static or linear. Therefore, EMD-based segmentation is an adaptive and signal-based segmentation. The analysed signal assumes the EMD-type overlaps the IMF drawn using the separation process. Traditional signal processing methods use predefined basic functions for analyzing EEG signals based on Fourier transitions and wavelengths, reducing the time-frequency. The secure linear support or apriori functions developed are only useful for static signals and may not be useful for investigating transient signals such as EEG. In biological systems, the frequency of oscillations cannot be determined. EEG rhythms revolve around different frequency ranges, allowing traditional methods such as pre-established Fourier and wavelet analyses. Some basic functions are not suitable for analysis of the EEG signal. For biomedical signals such as EEG, the EMD method achieves better localization of different frequency components  $\mu$ and $\beta$  of vary and rhythm between MI compared to methods based on short-term Fourier transform (STFT) [20] and wavelet transformer. The EMD scheme robotically breaks the x(t) signal into a refined IMF  $D_p(t)$ , which can be seen as a finite and symmetrical function. The symmetry of the IMF was examined for classification. Each drawn IMF must meet two basic situations: (i) The sum of hands and zero crossings should not be greater than or equal to one. The EMD procedure for signal x(t) can be précised in the subsequent test procedure:

**Phase 1:** Take one  $G_1(t) = x(t)$ .

**Phase 2:** Regulate the extrema of  $G_1(t)$ .

**Phase 3:** Calculate the down and upper envelopes  $E_{max}(t)$  and  $E_{min}(t)$ , correspondingly, by interpolating the maxima and minima correspondingly

**Phase 4:** Calculate the local mean  $asm(t) = (E_{max}(t) + E_{min}(t))/2$ .

**Phase 5:** Subtract m(t) from the unique signal as  $G_1(t) = G_1(t) - m(t)$ .

**Phase 6:** Check whether  $G_1(t)$  is an IMF by putting those mentioned above two basic situations of IMF.

**Phase 7:** Recap phase from (2) to (6) until an IMF  $g_1(t)$  is resolute.

When the initially determined the IMF, after considering a  $D_1(t) = G_1(t)$ , which can be deliberated in the minor temporal scale in x(t) signal. To regulate the residual IMF components, find the residue  $rs_1(t)$  of the data by subtracting  $D_1(t)$  from the signal as  $rs_1(t) = x(t) - D_1(t)$ . In the complete sifting course, the basic functions and the remains can be

stated as:

$$rs_1(t) - D_2(t) = rs_2(t), \dots, rs_{M-1}(t) - D_M(t) = rs_M(t)$$
 (4)

Where  $rs_M(t)$  is the last residue. At the termination of the complete sifting course, the signal x(t) can be conveyed as a linear grouping of IMFs and an excess as trails:

$$x(t) = \sum_{p=1}^{M} D_{p}(t) + rs_{M}(t)$$
 (5)

Where M is the amount of IMFs and  $rs_M(t)$  is the final residue.

#### Deep Forest

The output of EMD signals is given input for this classifier to predict the student's dyslexia level. The Deep Forest is an ensemble-based decision tree approach that emphasizes building deep models using modules that are non-differentiable. It is built around 3 major principles, which are the reasons behind deep models' rich accomplishments. The reasons are as follows:

Layer by Layer processing: It is considered one of the major factors since, no matter how complex the flat model becomes, the features of layer-by-layer processing cannot be achieved.

In-model feature transformation: Basic machine learning models work on the original features. However, new features are generated during the learning process of a deep model.

Appropriate model complexity: Because large datasets need complex models, basic machine learning models are limited in complexity. However, it is not the case with deep models.

The overall structural working of the deep forest is separated under two broad parts Cascade Forest Structure & Multi-Grained Scanning. A Cascade forest structure ensures layer-by-layer processing, while Multi-grained scanning allows the model to achieve sufficient complexity.

#### Cascade Forest Structure

A cascade structure is employed to represent the layer-by-layer processing of raw features. Each layer in the cascade takes input (processed information) from the previous layer and feeds it into the next layer. A layer in the structure can be defined as an ensemble of decision tree forests. It is ensured that diversity is maintained while creating ensembles by including different kinds of forests. This has also been depicted in Fig. 3.

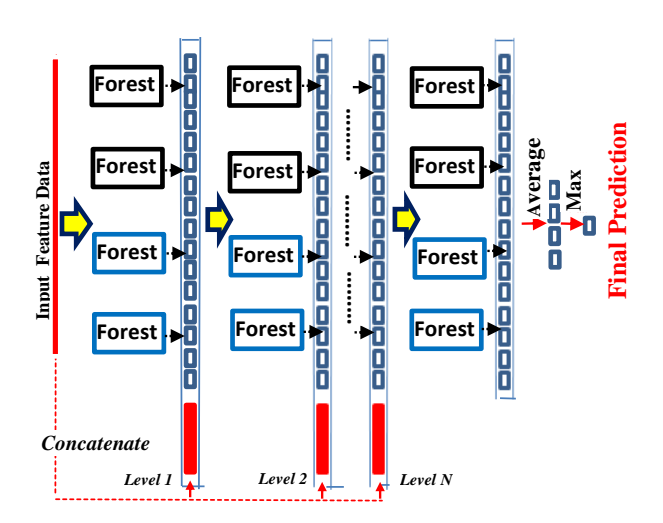


Fig. 3. Cascade forest construction

The working in cascading stage proceeds as follows, for a given case, an approximate class distribution will be generated by each forest. This is done by considering the training examples and fraction of different classes at the terminal or leaf node where the particular instance falls, followed by averaging across all the trees in the same forest. The approximated class distribution so obtained forms a vector of classes with the help of k-fold cross-validation. The vector is then concatenated with the original set of features. The result is then forwarded to the next cascading layer. K-fold cross-validation helps in reducing the hazard of overfitting. The number of levels is determined robotically based on the performance of the validation set

A striking difference between working deep forests and other deep models is the ability to adaptively change the model

complexity by terminating the amount of training data when tolerable. This provides a considerable advantage when working with datasets of varying sizes.

#### **Multi-Grained Scanning**

The cascading forest procedure is enriched with the procedure of multi-grained scanning. The inspiration behind the inclusion of the multi-grained scanning procedure was that deep models are generally well-suited and also good at handling feature relationships. The procedure is depicted in Fig. 4. The sliding windows and feature vectors scan raw features. The feature vectors are regarded as either negative or positive instances based on the extraction from the training sample;

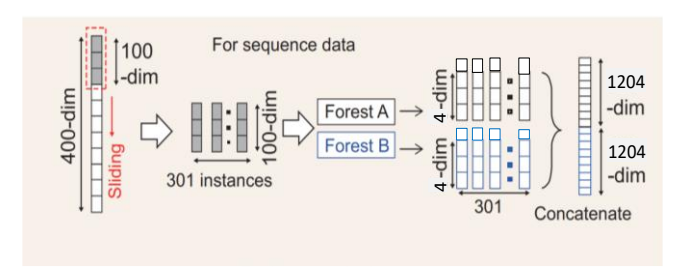


Fig. 4. .Multi-Grained scanning.

They are then used to produce class vectors. A completely random forest is trained using the instances extracted from windows of the same size. The concatenation of generated class vectors obtains transformed features.

The actual label of the training sample is used to assign the instances extracted from the windows. Though these assignments can be incorrect, they can be attributed to the flipping output method. Also, feature sampling can be performed if transformed feature vectors are too long. The sliding window size is varied to obtain different-grained feature vectors.

The Deep Forest has shown a lot of promise, and its success can be attributed to the following factors:

Fewer hyper-parameters

Data-dependent tuning of model's complexity

Less dependence on GPU

The scalable manner uses distributed parallel ML algorithms with several optimization strategies that enable it to manage large networks and host event volumes. The scalable design enables a quick and parallel examination of network and host-level actions using the overall graphic processing unit (GPU) processing capacity. Finally, this classifier can be able to identify dyslexia students.

#### Results and Discussion

A tgam1 module, dry electrode, and ear clip electrode collect the signals with the brain sense device. There is support for Bluetooth v2.1 class 2 (10-meter range) on iOS and Android. 60% of the data is used to train the classifier, and 40% is used for testing. The experimental scenarios use commercially available EEG units that interface with MATLAB software for data acquisition and control to provide real-time EEG signals.

#### Performance metrics

The basis truth value is necessary to evaluate the various statistical measures. The following four instances are used for calculating the performance metrics.

True Positive (TP) - the sum of students' records properly categorized to the normal class.

False Negative (FN) - the sum of students' records who have dyslexia is wrongly categorised to the normal class.

True Negative (TN) - the sum of students' records properly categorized to the dyslexia class.

False Positive (FP) - the sum of normal students wrongly categorized to the dyslexia class.

The following evaluation metrics are examined based on the above-given terms.

**Accuracy:** The ratio of the predictable connection records to the whole test dataset is estimated. If the precision is higher, then the model of ML is better (Accuracy BE [0,1]). Accuracy is an appropriate metric for an experimental dataset with balanced classes.

**Precision:** It guesses the ratio of correctly identified attachment logs to the number of all identified attachments. The ML model is better with higher precision (Precision [0,1]).

**F1-Score:** F1-Score is known as F1-Score, too. It is precise and recalls the harmonic mean. The greater the F1-score, the better (F1-00score for [0,1]).

**False Positive Rate (FPR)** calculates the ratio of normal linking records to the number of standard connection records as attacks. The lower FPR will improve the model for ML (FPR [0,1]).

Performances evaluation of the Proposed Model

In this section, the proposed DFC is tested with various existing techniques regarding Accuracy, precision, recall, and F-score, tabulated in Table II and Fig. 5.

TABLE II. COMPARATIVE ANALYSIS OF PROPOSED DFC WITH EXISTING TECHNIQUES

Algorith m	Accu racy	Preci sion	Rec all	F- score
KNN	92.10	92.43	92.1 5	91.68
DT	92.46	93.48	92.4 4	91.81
SVM	89.52	90.21	89.5 4	89.03
RNN	94.53	96.61	92.5 2	92.24
LSTM	94.16	96.17	92.3 2	92.10
Proposed -Deep Forest Classifier {DFC)	95.62	98.32	94.6	94.53

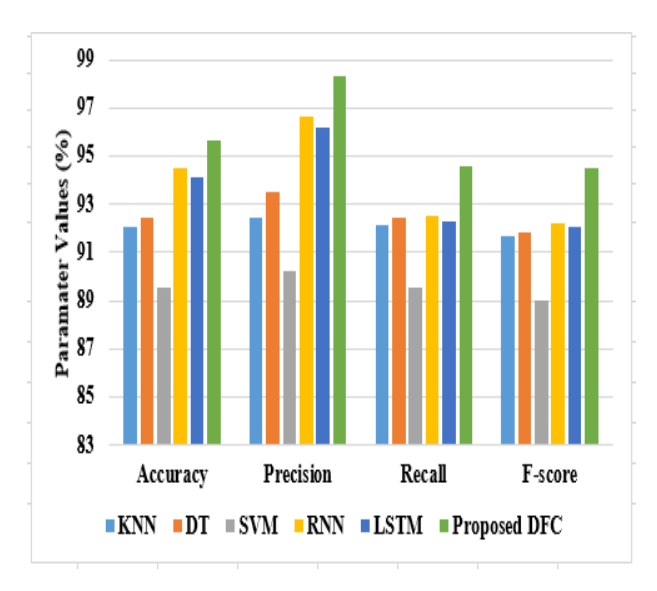


Fig. 5. Graphical Representation of Proposed DFC with various ML and DL techniques

In the accuracy experiments, the existing techniques, such as KNN and DT, achieved nearly 92%, RNN and LSTM achieved nearly 94%, SVM achieved 89.52%, and the proposed DFC achieved 95.62% accuracy. This shows that the performance of the proposed DFC is better than existing techniques. Like Accuracy, the existing techniques such as RNN, LSTM, KNN, and DT achieved nearly 92% of recall, SVM achieved 89.54% of recall, and proposed DFC achieved 94.62% of recall values. The existing techniques, such as KNN and DT, achieved nearly 91% of F-measure, RNN, LSTM nearly 92% of F-measure,

SVM achieved 89.03%, and proposed DFC achieved 94.53% of F-measure. The existing techniques and proposed classifiers are implemented with SSA-EMD, SSA, and EMD for performance analysis and to detect dyslexia patients from the normal class category. Accuracy is calculated for all techniques to test their efficiency and is provided in Table III and Fig. 6.

## TABLE III. VALIDATED ANALYSIS OF THE PROPOSED MODEL WITH EXISTING TECHNIQUES IN TERMS OF ACCURACY

	Accuracy (%)			
Algorithm	SSA-EMD	Direct EMD	Direct SSA	
KNN	90.82	92.43	89.79	
DT	92.44	93.12	90.41	
SVM	92.13	93.26	92.27	
RNN	94.63	96.16	92.66	
LSTM	96.63	94.37	91.99	
Proposed Deep Forest Classifier	97.89	94.23	94.13	

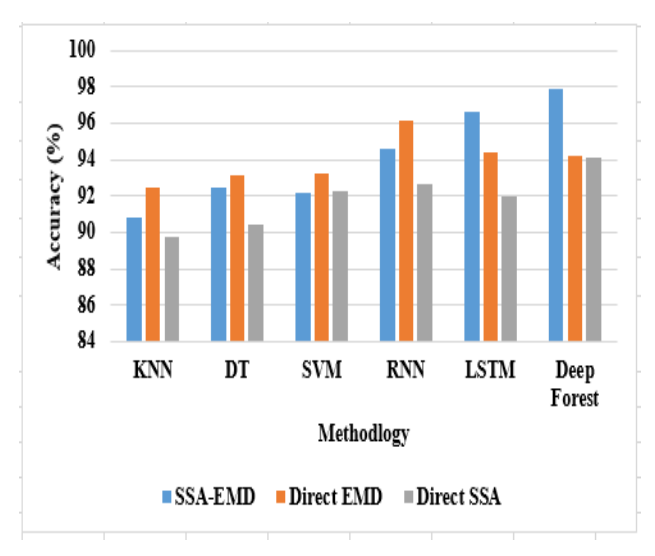


Fig. 6. Graphical Representation of Proposed DFC in terms of Accuracy

From the graph itself, it is proved that DFC achieved 97.89% accuracy only while implemented with SSA-EMD. Where only EMD is used, it achieved 94.23% accuracy and 94.13% accuracy only DFC is implemented with SSA. Among the existing techniques, KNN achieved very poor performance, i.e., 90.82% accuracy with SSA-EMD, 93.43% Accuracy with EMD and 89.79% with SSA. The above table proves that the existing techniques didn't perform much better on SSA and EMD than on SSA-EMD. Therefore, the impact of SSA-EMD is high only on proposed DFC and accurately predicts the dyslexia patients from the normal category.

#### 2. CONCLUSION

Those with dyslexia have to deal with numerous educational obstacles in daily life. People with dyslexia face challenges such as difficulties in academic settings, being mistreated and receiving negative feedback on their behavior, and being unable to obtain adequate support to help them overcome these challenges. This project aims to help dyslexics overcome their challenges by using adaptively sensed behavior. We, therefore, use a deep learning strategy based on DFC to anticipate students' dyslexia concerning the learning material. The input signals are collected from 15 students with dyslexia and normal-category people. The experiments use the DL and existing ML techniques with SSA-EMD, SSA, and EMD for

## Dr. Vishal Patil1, Dr. Bajirao Shirole , Dr. Rajiv R. Bhandari, Dr. Sharmila Zope, M.D. Sanap , Dr. Vijay More, Vijay Bodake, Dr. R. Ramkumar

accuracy comparison. The results proved that the proposed DFC achieved better performance while implementing both SSA-EMD and achieved 98% accuracy.

In contrast, the existing DL techniques achieved nearly 95% to 96% accuracy with the SSA-EMD technique. This is due to the functionality of the parameters that influence the input parameters. In future work, the performance of the proposed DFC classifier can be further enhanced by modifying it using efficient optimization techniques for predicting dyslexia disorder.

#### REFERENCES

- [1] M. I.-A.-B. Ibn-Qaiyim al-Ğauzīya, *Prophetic Medicine:* = *Aţ-Ţibb an-nabawī*, 2nd ed. New Delhi: Islamic Book Service, 2003.
- [2] M. Dalli, O. Bekkouch, S.-E. Azizi, A. Azghar, N. Gseyra, and B. Kim, 'Nigella sativa L. Phytochemistry and Pharmacological Activities: A Review (2019-2021)', *Biomolecules*, vol. 12, no. 1, p. 20, Dec. 2021, doi: 10.3390/biom12010020.
- [3] Z. Albakry *et al.*, 'A comparative study of black cumin seed (Nigella sativa L.) oils extracted with supercritical fluids and conventional extraction methods', *Journal of Food Measurement and Characterization*, vol. 17, no. 3, pp. 2429–2441, Jun. 2023, doi: 10.1007/s11694-022-01802-7.
- [4] N. AlFraj and A. Hamo, 'Evaluation of technical efficiency of some rain-fed cereal and legume crops production in Syria: does crisis matter?', *Agric & Food Secur*, vol. 11, no. 1, p. 49, Oct. 2022, doi: 10.1186/s40066-022-00389-y.
- [5] S. Ekren, I. C. Paylan, and A. Gokcol, 'Seed quality improvement applications in black cumin seeds (Nigella sativa L.)', *Front. Sustain. Food Syst.*, vol. 7, p. 1212958, Aug. 2023, doi: 10.3389/fsufs.2023.1212958.
- [6] Y. Kabir, Y. Akasaka-Hashimoto, K. Kubota, and M. Komai, 'Volatile compounds of black cumin (Nigella sativa L.) seeds cultivated in Bangladesh and India', *Heliyon*, vol. 6, no. 10, p. e05343, Oct. 2020, doi: 10.1016/j.heliyon.2020.e05343.
- [7] S. Hussain *et al.*, 'Phytochemical profile, nutritional and medicinal value of Nigella sativa', *Biocatalysis and Agricultural Biotechnology*, vol. 60, p. 103324, Sep. 2024, doi: 10.1016/j.bcab.2024.103324.
- [8] M. Umer *et al.*, 'Nigella sativa for the treatment of COVID-19 patients: A rapid systematic review and metaanalysis of randomized controlled trials', Food Science & Nutrition, vol. 12, no. 3, pp. 2061–2067, Mar. 2024, doi: 10.1002/fsn3.3906.
- [9] A. Ahmad *et al.*, 'A review on therapeutic potential of Nigella sativa: A miracle herb', *Asian Pac J Trop Biomed*, vol. 3, no. 5, pp. 337–352, May 2013, doi: 10.1016/S2221-1691(13)60075-1.
- [10] A. Tero-Vescan, R. Ştefănescu, T.-I. Istrate, and A. Puşcaş, 'Fructose-induced hyperuricaemia protection factor or oxidative stress promoter?', *Natural Product Research*, pp. 1–13, Mar. 2024, doi: 10.1080/14786419.2024.2327624.
- [11] L. Li, Y. Zhang, and C. Zeng, 'Update on the epidemiology, genetics, and therapeutic options of hyperuricemia', *Am J Transl Res*, vol. 12, no. 7, pp. 3167–3181, 2020.
- [12] P. Zhang *et al.*, 'Dietary intake of fructose increases purine de novo synthesis: A crucial mechanism for hyperuricemia', *Front. Nutr.*, vol. 9, p. 1045805, Dec. 2022, doi: 10.3389/fnut.2022.1045805.
- [13] M. Halimulati *et al.*, 'Anti-Hyperuricemic Effect of Anserine Based on the Gut-Kidney Axis: Integrated Analysis of Metagenomics and Metabolomics', *Nutrients*, vol. 15, no. 4, p. 969, Feb. 2023, doi: 10.3390/nu15040969.
- [14] M. Rashid *et al.*, 'Silver Nanoparticles from Saudi and Syrian Black Cumin Seed Extracts: Green Synthesis, ADME, Toxicity, Comparative Research, and Biological Appraisal', *Journal of Pharmacy and Bioallied Sciences*, vol. 15, no. 4, pp. 190–196, Oct. 2023, doi: 10.4103/jpbs.jpbs\_381\_23.
- [15] Nutrient Requirements of Laboratory Animals,: Fourth Revised Edition, 1995. Washington, D.C.: National Academies Press, 1995, p. 4758. doi: 10.17226/4758.
- [16] R. J. Johnson, T. Nakagawa, D. Jalal, L. G. Sanchez-Lozada, D.-H. Kang, and E. Ritz, 'Uric acid and chronic kidney disease: which is chasing which?', *Nephrology Dialysis Transplantation*, vol. 28, no. 9, pp. 2221–2228, Sep. 2013, doi: 10.1093/ndt/gft029.
- [17] R. Dangarembizi, K. H. Erlwanger, C. Rummel, J. Roth, M. T. Madziva, and L. M. Harden, 'Brewer's yeast is a potent inducer of fever, sickness behavior and inflammation within the brain', *Brain, Behavior, and Immunity*, vol. 68, pp. 211–223, Feb. 2018, doi: 10.1016/j.bbi.2017.10.019.
- [18] Y. Andriana *et al.*, 'Chemometric analysis based on GC-MS chemical profiles of essential oil and extracts of black cumin (Nigella sativa L.) and their antioxidant potentials', *J Appl Pharm Sci*, 2023, doi:

#### 10.7324/JAPS.2023.151774.

- [19] S. Wen *et al.*, 'An improved UPLC method for determining uric acid in rat serum and comparison study with commercial colorimetric kits', *Acta Chromatographica*, vol. 31, no. 3, pp. 201–205, Sep. 2019, doi: 10.1556/1326.2018.00449.
- [20] C. M. M. R. Barros *et al.*, 'SUBSTITUTION OF DRINKING WATER BY FRUCTOSE SOLUTION INDUCES HYPERINSULINEMIA AND HYPERGLYCEMIA IN HAMSTERS', *Clinics*, vol. 62, no. 3, pp. 327–334, Jun. 2007, doi: 10.1590/S1807-59322007000300019.
- [21] C. M. M. R. Barros *et al.*, 'SUBSTITUTION OF DRINKING WATER BY FRUCTOSE SOLUTION INDUCES HYPERINSULINEMIA AND HYPERGLYCEMIA IN HAMSTERS', *Clinics*, vol. 62, no. 3, pp. 327–334, Jun. 2007, doi: 10.1590/S1807-59322007000300019.
- [22] H. Zhou *et al.*, 'Hyperuricemia research progress in model construction and traditional Chinese medicine interventions', *Front Pharmacol*, vol. 15, p. 1294755, 2024, doi: 10.3389/fphar.2024.1294755.
- [23] P. J. Vento, M. E. Swartz, L. B. Martin, and D. Daniels, 'Food intake in laboratory rats provided standard and fenbendazole-supplemented diets', *J Am Assoc Lab Anim Sci*, vol. 47, no. 6, pp. 46–50, Nov. 2008.
- [24] H. Mashayekhi-Sardoo, R. Rezaee, and G. Karimi, 'Nigella sativa (black seed) safety: an overview', Asian Biomedicine, vol. 14, no. 4, pp. 127–137, Aug. 2020, doi: 10.1515/abm-2020-0020.
- [25] P. S, R. R, and K. R, 'Blood sample collection in small laboratory animals', *Journal of Pharmacology and Pharmacotherapeutics*, vol. 1, no. 2, pp. 87–93, Dec. 2010, doi: 10.4103/0976-500X.72350.
- [26] J. Zhao, 'A simple, rapid and reliable high performance liquid chromatography method for the simultaneous determination of creatinine and uric acid in plasma and urine', *Anal. Methods*, vol. 5, no. 23, p. 6781, 2013, doi: 10.1039/c3ay41061g.
- [27] Amtul Hafeez, Abdul Mudabbir Rehan, Zunera Hakim, Attiya Munir, Rabia Naseer Khan, and Aamna Khokhar, 'Nigella sativa Seeds Protective Ability in Pyrazinamide Induced Hyperuricemia in Mice', *Proceedings S.Z.M.C*, vol. 36, no. 1, pp. 44–48, Feb. 2022, doi: 10.47489/PSZMC-825361-44-48.
- [28] Y. Tayama, K. Sugihara, S. Sanoh, K. Miyake, S. Kitamura, and S. Ohta, 'Xanthine oxidase and aldehyde oxidase contribute to allopurinol metabolism in rats', *J Pharm Health Care Sci*, vol. 8, no. 1, p. 31, Dec. 2022, doi: 10.1186/s40780-022-00262-x.
- [29] M. Martin Fabritius, A. Broillet, S. König, and W. Weinmann, 'Analysis of volatiles in fire debris by combination of activated charcoal strips (ACS) and automated thermal desorption—gas chromatography—mass spectrometry (ATD/GC–MS)', *Forensic Science International*, vol. 289, pp. 232–237, Aug. 2018, doi: 10.1016/j.forsciint.2018.05.048.
- [30] X. Wei, I. Koo, S. Kim, and X. Zhang, 'Compound identification in GC-MS by simultaneously evaluating the mass spectrum and retention index', *Analyst*, vol. 139, no. 10, pp. 2507–2514, 2014, doi: 10.1039/C3AN02171H.
- [31] J. Nickel *et al.*, 'SuperPred: update on drug classification and target prediction', *Nucleic Acids Research*, vol. 42, no. W1, pp. W26–W31, Jul. 2014, doi: 10.1093/nar/gku477.